Martin, *Polym. Prepr., Am. Chem. Soc., Div. Polym. Chem.*, **15**(2), 8 (1974).
(11) G. Leiser, E. W. Fischer, and K. Ibel, *J. Polym. Sci., Polym. Lett.*, **13**, 39 (1975).
(12) R. G. Kirste, *Makromol. Chem.*, **101**, 91 (1967).
(13) D. Y. Yoon and P. J. Flory, *Polymer*, **16**, 645 (1975).
(14) Y. Fujiwara and P. J. Flory, *Macromolecules*, **3**, 288 (1970).
(15) See ref 2, pp 309–311.
(16) A. Abe, R. L. Jernigan, and P. J. Flory, *J. Am. Chem. Soc.*, **88**, 631 (1966).
(17) P. J. Flory, *Macromolecules*, **7**, 381 (1974).
(18) D. Y. Yoon and P. J. Flory, *J. Chem. Phys.*, **61**, 5366 (1974).
(19) See ref 2, pp 165–172.
(20) J. E. Mark and P. J. Flory, *J. Am. Chem. Soc.*, **88**, 3702 (1966).
(21) D. Y. Yoon, P. R. Sundararajan, and P. J. Flory, *Macromolecules*, **8**, 776 (1975).
(22) P. J. Flory, P. R. Sundararajan, and L. C. DeBolt, *J. Am. Chem. Soc.*, **96**, 5015 (1974).
(23) H. Durchschlag, O. Kratky, J. W. Breitenbach, and B. A. Wolf, *Monatsh. Chem.*, **101**, 1462 (1970).
(24) H. Durchschlag, G. Puchwein, O. Kratky, J. W. Breitenbach, and O. F. Olaj, *J. Polym. Sci., Part C*, **31**, 311 (1970).
(25) D. Y. Yoon and P. J. Flory, in preparation.
(26) L. F. Johnson, F. Heatley, and F. A. Bovey, *Macromolecules*, **3**, 175 (1970).
(27) See ref 2, pp 307–314.
(28) A. Abe, in preparation.
(29) NOTE ADDED IN PROOF: Since this paper was submitted, we have learned that similar calculations on polymethylene chains have been carried out by Z. Zierenberg, D. K. Carpenter, and J. H. Hsieh. Our results are in agreement with theirs, which will appear in the *J. Polym. Sci., Polym. Symp.*

II. Small-Angle Neutron and X-Ray Scattering by Poly(methyl methacrylate) Chains

D. Y. Yoon and P. J. Flory*

Department of Chemistry, Stanford University, Stanford, California 94305.
Received December 2, 1975

ABSTRACT: Scattering functions describing the angular dependence of the intensity of radiation scattering by poly(methyl methacrylate) (PMMA) chains are calculated on the basis of an appropriate rotational isomeric state model. Numerical calculations are carried out, with main emphasis on the range $0.05 < \mu < 0.5$ Å^{-1}, where $\mu = (4\pi/\lambda) \sin(\vartheta/2)$, by evaluating $\langle(\mu r_{ij})^{-1} \sin(\mu r_{ij})\rangle$ for pairs of scattering groups i and j as the averages for 1000 Monte Carlo chains. Errors incident upon truncation of series expansions of this quantity for large magnitudes of the scattering vector μ are thus avoided. The theoretical scattering function $F_x(\mu) \propto I\mu^2$ exhibits two maxima, in harmony with experimental results of Kirste on small-angle x-ray scattering by syndiotactic PMMA chains in solution. The point scatterer approximation according to which the scattering by each repeating unit is identified with the location of the α carbon is inappropriate for neutron scattering by *H*-PMMA dispersed in *D*-PMMA host. Calculations for separate scattering loci centered in CH_3 and CH_2 groups differ considerably at large μ from those carried out in the point scatterer approximation. They are in good agreement with experimental neutron scattering results. Thus, the validity of the rotational isomeric state analysis for comparatively short chain sequences is demonstrated.

In a recent paper[1] we presented theoretical computations on the intensity of radiation scattering by poly(methyl methacrylate) (PMMA) as a function of scattering angle ϑ over the range $0 < \mu < 0.3$ Å^{-1}, where $\mu = (4\pi/\lambda) \sin(\vartheta/2)$. The calculations were carried out according to eq 4 of the preceding paper[2] truncated at g_8. The required moments were computed on the basis of a rotational isomeric state scheme that is in harmony with the geometric characteristics and steric constraints in the PMMA chain and with detailed calculations of its conformational energy.[3] The theoretical scattering function $F_x(\mu)$, which is proportional to $I\mu^2$, where I is the scattering intensity, was found to increase monotonically with μ for isotactic PMMA. For predominantly syndiotactic PMMA, however, the calculated $F_x(\mu)$ exhibited a maximum at $\mu \approx 0.05$ Å^{-1} and a minimum at $\mu \approx 0.18$ Å^{-1}. These features of the variation of $F_x(\mu)$, or of $I\mu^2$, with μ and their dependence on the stereochemical configuration of PMMA were found to be in satisfactory qualitative agreement with the experimental results of small-angle neutron and x-ray scattering by PMMA chains in bulk and in solution, respectively, as reported by Kirste and co-workers.[4–6] The unusual appearance of a maximum in $F_x(\mu)$ had been misconstrued as evidence of helical sequences in solution or of ordered regions in the bulk polymers. In our previous paper[1] this maximum was shown, on the contrary, to be a direct consequence of the preference of racemic dyads of PMMA for the trans,trans conformation in the random coiled state together with the inequality of the skeletal bond angles at $-CH_2-$ and at the disubstituted C^α atom.

With respect to quantitative treatment of scattering in the range $\mu > \sim 0.10$ Å^{-1}, however, the preliminary calculations[1] are deficient in two respects: (i) truncation of the series expansion of the scattering function $F_x(\mu)$ at terms in $\langle r_t^8\rangle$ (see eq 4 of the preceding paper,[2] referred to hereafter as I), and (ii) representation of the repeating unit

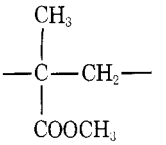

as a point scatterer located at the C^α atom. The latter approximation is especially inappropriate for neutron scattering by protonated (or deuterated) PMMA dispersed in a deuterated (or protonated) PMMA host. The scattering length of the CD_2 group for coherent scattering of neuterons is large compared to the vanishingly small value for CH_2. The distinction between deuterons and protons (or vice versa) therefore is the principal source of contrast, and hence these atoms (H or D) are the main loci of scattering. The methylene and methyl groups in which they are situated are appreciably displaced from C^α.

The point scatterer approximation should be more appropriate for small-angle x-ray scattering by PMMA chains in a solvent where the contrast in electron density between

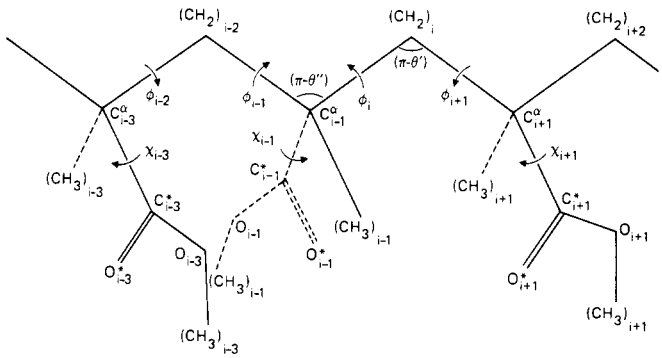

Figure 1. The syndiotactic PMMA chain in the all-trans conformation.

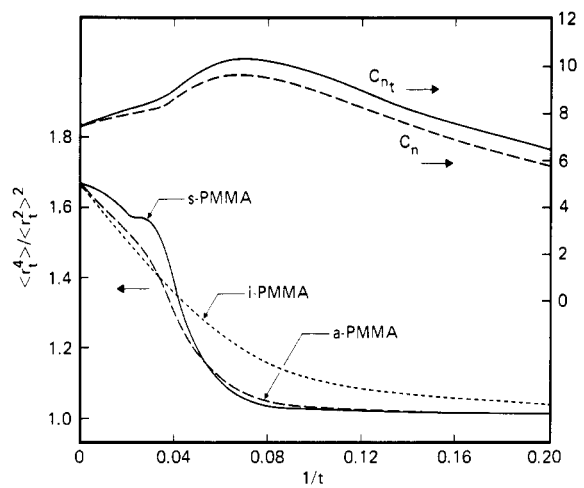

Figure 2. Characteristic ratios $C_{n_t} = \langle r_t^2\rangle/2t\ell^2$ for sequences of t units centered within syndiotactic PMMA chains of $100 + t + 100$ units, and $C_n = \langle r_n^2\rangle/n\ell^2$ for chains comprising a total of $n = 2t$ bonds plotted against $1/t$ or $2/n$ (right-hand ordinate scale). Also, ratios $\langle r_t^4\rangle/\langle r_t^2\rangle^2$ calculated for sequences of t units centered within a chain of $200 + t$ units plotted against $1/t$ (left-hand ordinate scale).

the dispersed polymer and the surrounding medium is responsible for the scattering. The center of electron density within a repeating unit lies close to its α-carbon atom.

In this paper we present theoretical calculations intended to overcome the deficiencies of the previous, preliminary investigation.[1] The calculations reported here are confined to syndiotactic PMMA inasmuch as the available experimental results, both from the x-ray scattering of dilute solutions and from the neutron scattering by *H*-PMMA dispersed in *D*-PMMA, have been obtained on polymers that were predominantly syndiotactic. We first present calculations that overcome the limitation (i) of truncation of the series expansion in eq I-4 at g_8, the point scatterer approximation (ii) being retained. These calculations are pertinent to small-angle x-ray scattering. Calculations, addressed mainly to small-angle neutron scattering, are then presented in which the principal scattering groups within each repeating unit are separately considered.

Chain Structure and Configurational Statistics

The structure of the PMMA chain is shown in Figure 1. The skeletal bond angle at CH_2 is strained by severe steric interactions due to the presence of two substituents.[7] As in related investigations[1,3] of PMMA, we assign values[8] of 58 and 70° to the respective angles θ' and θ'' defined in Figure 1, and take $\ell = 1.53$ Å for the bond length. Impingements

Table I
Conformational Probabilities for Bonds within Long Syndiotactic PMMA Chains at $T = 300$ K

	Bond pair flanking C^α	Dyad bond pair
$p_t = 1 - p_g$	0.942	0.942
p_{tt}	0.883	0.887
$p_{tg} = p_{gt}$	0.058	0.055
p_{gg}	0.000	0.003
q_{tt}	0.938	0.942
q_{tg}	0.062	0.058
q_{gt}	1.000	0.942
q_{gg}	0.000	0.058

of atoms of the ester group on neighboring methylene groups limit rotations about the C^α–CO bond to small ranges in which the plane of the ester group is approximately perpendicular to the plane of the skeletal bonds flanking C^α.[3] Gauche bar ($\bar{g}$) rotations, for which $\varphi = -120°$ in the conventions relating rotational sense to bond chirality set forth in ref 9, place C^α syn to both $COOCH_3$ and CH_2. In this conformation the trans planar ester group (see Figure 1) is subjected to severe steric overlaps that virtually preclude conformations throughout the $\bar{g}$ domain.[3] Hence, two rotational states, trans (t) and gauche (g) at $\varphi = 0$ and 120°, respectively, suffice for representation of the accessible conformations of the chain. Elements of the statistical weight matrices, of 2×2 order, are determined by two parameters, α and β, previously defined and evaluated.[3] A priori probabilities p_ξ and $p_{\xi\eta}$ and conditional probabilities $q_{\xi\eta}$ used in the Monte Carlo calculations are listed in Table I. The latter probabilities were calculated from the former ones using eq I-6. All values are for a temperature of 300 K.

Scalar Moments of the Chain Vector r

The even moments $\langle r_t^{2p}\rangle$ up to $\langle r_t^8\rangle$ for syndiotactic, isotactic, and "atactic" (meso fraction $w_m = 0.2$) PMMA chains of t units situated within long chains were calculated using the procedures described previously.[10,11] In Figure 2 the characteristic ratio $C_{n_t} = \langle r_t^2\rangle/2t\ell^2$ for a sequence of t repeating units ($n = 2t$ skeletal bonds) centered within a chain of $t + 200$ units is shown by the solid line as a function of $1/t$ for syndiotactic PMMA. The dashed line represents the characteristic ratio C_n for syndiotactic PMMA chains having a total of n bonds. The small difference between the values of C_{n_t} and C_n for syndiotactic PMMA shown in Figure 2, and the even smaller differences for isotactic and for atactic PMMA according to calculations not shown, confirm previous indications[12] that the configuration-dependent characteristics of a sequence of bonds usually are little affected by units adjoining the sequence.

Curves showing $\langle r_t^4\rangle/\langle r_t^2\rangle^2$ for isotactic, syndiotactic, and atactic PMMA as a function of $1/t$ are included in Figure 2. The ratios $\langle r_t^6\rangle/\langle r_t^2\rangle^3$ and $\langle r_t^8\rangle/\langle r_t^2\rangle^4$ for isotactic and syndiotactic PMMA are presented in Figure 3. The latter ratio is reduced by the factor $\frac{1}{3}$ in order to render its intercept ($\frac{35}{3}$) coincident with that for the former ($\frac{35}{9}$). The decreases in these ratios with $1/t$ are indicative of departures from the Gaussian distribution, which is reached in the limit $1/t \to 0$.

Calculations of $F_x(\mu)$ in the Point Scatterer Approximation

Results of calculations carried out under the assumption that the scattering by a given repeating unit is centered at the α carbon of that unit are presented in Figure 4. All

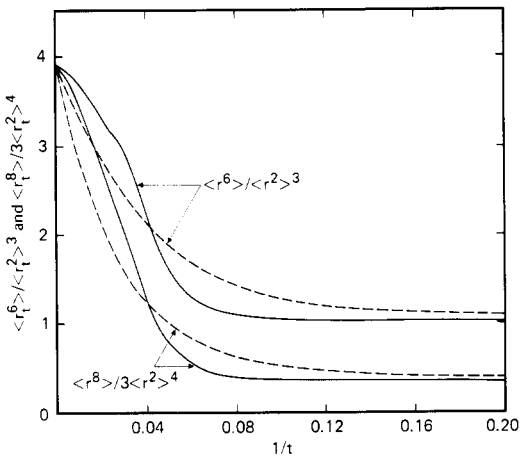

Figure 3. Ratios $\langle r_t^6\rangle/\langle r_t^2\rangle^3$ and $\langle r_t^8\rangle/\langle r_t^2\rangle^4$ for isotactic (dashed line) and syndiotactic (solid line) PMMA sequences of t units centered within chains of $t + 200$ units plotted against $1/t$.

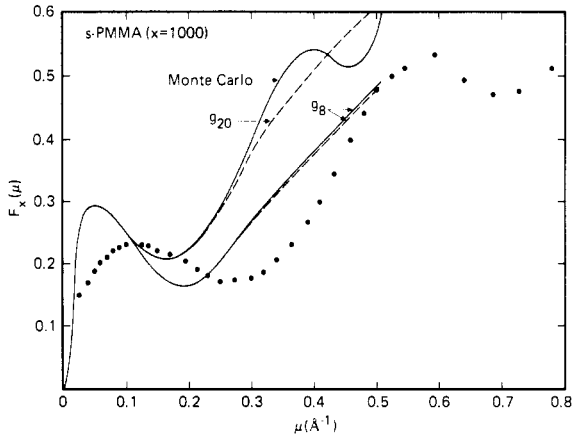

Figure 4. The scattering function $F_x(\mu)$ for syndiotactic PMMA chains of 1000 monomer units computed in the point scatterer approximation. The various curves differ in the methods used to evaluate $\langle(\mu r_t)^{-1}\sin(\mu r_t)\rangle$: eq I-4 truncated at g_8 and g_{20} for the curves so labeled, the required moments being calculated algebraically (solid g_8 curve) or by Monte Carlo methods (dashed curves); upper solid curve by direct Monte Carlo computation for $t \leq 30$ units; see text. The points represent experimental data obtained by Kirste[4,5] from the x-ray scattering by a dilute solution of PMMA in benzene; reproduced from Figure 10 of ref 5.

curves are for a syndiotactic chain of $x = 1000$ units. The lower solid curve was calculated according to eq I-4 of the preceding paper[2] with the series therein truncated at g_8; the polynomials $g_{2;t} \ldots g_{8;t}$ were obtained from the moment calculations above. This curve and corresponding ones for atactic ($w_m = 0.20$) and isotactic ($w_m = 1.00$) PMMA have been published previously.[1] The scattering function for the atactic polymer also exhibits a maximum; it is less pronounced than for the syndiotactic ($w_m = 0$) polymer and displaced toward smaller values of μ. The scattering function for isotactic PMMA is monotone with μ.[1] It resembles polystyrene in this respect; see Figure 8 of the preceding paper (I).[2]

The scattering function expanded in the polynomials $g_{2p;t}$, as in eq I-4, fails to converge at $g_{8;t}$ for $\mu > 0.10$ Å^{-1}. The curve labeled g_8 in Figure 4 becomes inaccurate on this account at larger values of μ. Accordingly, terms $\langle(\mu r_t)^{-1}\sin(\mu r_t)\rangle$ were evaluated by Monte Carlo calculations for $t \leq 30$ units, 1000 Monte Carlo chains being generated for each t over this range (see I). Contributions of sequences $t > 30$ to the total scattering are negligible for $\mu > 0.10$ Å^{-1}. This was demonstrated by Monte Carlo calculations covering the range up to $t = 100$ units. Sequences with $t > 30$, which assume importance only for $\mu < 0.10$ Å^{-1}, are well represented by the series expansion in eq I-4 truncated at $g_{8;t}$. Hence, following the procedure employed in I, we divide the sum over t into terms for $t \leq 30$ and those for $t > 30$. The former are evaluated according to eq I-3 from the Monte Carlo averages mentioned, and the latter from the moments $\langle r_t^2\rangle$ to $\langle r_t^8\rangle$ using eq I-4 with the series truncated at g_8. The upper solid curve in Figure 4 has been evaluated in this manner.

The lower dashed curve in Figure 4, like the solid "g_8" curve, was calculated from eq I-4 with the series terminated at g_8. Unlike the solid curve, the moments $\langle r_t^2\rangle \ldots \langle r_t^8\rangle$ for $t \leq 30$ used for calculation of the dashed curve were obtained from the Monte Carlo chains used above; for $t > 30$ the "exact" moments shown in Figures 2 and 3 were used, these having been computed algebraically[11] as pointed out above. The virtual coincidence of the two g_8 curves demonstrates the essential consistency of the two methods of calculation. Effects of the finite sizes of the Monte Carlo samples appear not to be significant.

The dashed curve labeled "g_{20}" was calculated similarly. For $t \leq 30$, Monte Carlo moments were used and the series in eq I-4 was truncated at g_{20}. For $t > 30$, moments calculated algebraically (Figures 2 and 3) were used, the series in eq I-4 being terminated at g_8. Beyond $\mu = 0.15$ Å^{-1} this curve rises much above those calculated using terms only up to g_8 for all t. It thus demonstrates the inadequacy of convergence at g_8 for larger μ. By comparison of the "g_{20}" and "Monte Carlo" curves, failure to converge at g_{20} is indicated beyond $\mu = 0.30$ Å^{-1}.

The experimental small-angle x-ray scattering results reported by Kirste[4,5] for syndiotactic PMMA dissolved in benzene are represented by the points included in Figure 4.[17] Like the "Monte Carlo" curve, they display two maxima. The observed maxima occur at somewhat larger values of μ than those exhibited by the calculated curve: at ca. 0.11 vs. ca. 0.05 Å^{-1} and at ca. 0.57 vs. 0.40 Å^{-1}, respectively. Otherwise, the curve described by the points and the one calculated are remarkably similar. The second maximum occurs at about twice the ordinate of the first in each plot. Differences in locations of the calculated and observed maxima may reflect inaccuracies of the rotational isomeric state model[3] as well as comparatively large experimental errors inevitable for larger values of μ. The outer maximum in the calculated curve should be especially vulnerable to inaccuracies arising from the point scatterer approximation and from correlations with neighboring solvent molecules, ignored altogether in the calculations.

The similarity of the calculations carried out in the highest approximation, involving direct (Monte Carlo) evaluation of $\langle(\mu r_t)^{-1}\sin(\mu r_t)\rangle$ for $t \leq 30$, to Kirste's results confirms the adequacy of the point scatterer approximation for the treatment of scattering by x-rays, up to $\mu = 0.3$ Å^{-1} at least. As we have pointed out in our earlier paper,[1] the maximum in the characteristic ratio for syndiotactic PMMA (see Figure 2) at $t \approx 15$ units and the similar maximum for "atactic" PMMA with $w_m \approx 0.2$ (shown in Figure 1 of ref 1) are mainly responsible for the appearance of maxima at $\mu \approx 0.05$–0.11 Å^{-1} in the calculated scattering function $F_x(\mu)$, and in $I\mu^2$ as measured experimentally by x-ray and neutron scattering.[4-6] These maxima, occurring in both C_{n_t} and $F_x(\mu)$, are attributable[1] to the inequality of the skeletal bond angles at C^α and CH_2 and to the strong preference of racemic dyads for the trans,trans conformation.[1] This preference is more pronounced in the syndiotactic than in the isotactic PMMA chains. It is illustrated by

calculations showing that the average length of sequences over which $|tt|$ dyad conformations are perpetuated is about nine units for syndiotactic PMMA, compared to only about three units in the isotactic chain.[1]

Consistent with this interpretation is the fact that $F_x(\mu)$ calculated for isotactic PMMA increases monotonically with μ (see Figures 2 and 3 of ref 1), and this is in harmony with experimental x-ray scattering results of Kirste.[5] Thus, the influence of stereochemical structure is correctly represented by the model.

The source of the second maximum has not been identified.

Neutron Scattering by Deuterated PMMA

Elaborating eq I-4 to take account of several scattering loci in each repeating unit, we obtain

$$F_x(\mu) = \sum_{k,\ell} f_k f_\ell \left[\frac{\mu^2 \sin(\mu r_{0;k\ell})}{\mu r_{0;k\ell}} + 2\mu^2(x+1)^{-1} \sum_{t=1}^{x} (x+1-t) \left\langle \frac{\sin(\mu r_{t;k\ell})}{\mu r_{t;k\ell}} \right\rangle \right] \Big/ \sum_{k,\ell} f_k f_\ell \quad (1)$$

where f_k and f_ℓ are the scattering factors for groups k and ℓ, respectively; $r_{t;k\ell}$ is the distance between a group k in a given unit and a group ℓ in the tth following unit; $r_{0;k\ell}$ is the distance between groups k and ℓ in the same monomer unit. In the case of neutron scattering by mixtures of protonated and deuterated PMMA, where the difference between H and D accounts for most of the scattering, each repeating unit may be represented by three scattering loci situated respectively at the centers of the H (or D) atoms in each of the two CH_3 groups and at the center of the CH_2 group. The relative scattering factors are 3 and 2.

The contribution of each pair k,ℓ of scattering groups separated by $t \leq 30$ units to the total scattering was calculated according to eq 1 by evaluating $\langle (\mu r_{t;k\ell})^{-1} \sin(\mu r_{t;k\ell}) \rangle$ as the average over 1000 Monte Carlo chains. For $t > 30$, the scattering attributable to each of the pair of units was centered at its C^α atom and the combined contributions of these more remote pairs were calculated as above by executing the summation in eq I-4 commencing at $t = 31$, the summation being truncated at g_8. The theoretical scattering function $F_x(\mu)$ for syndiotactic PMMA was evaluated in this manner as a function of μ.

In experiments on the scattering by a protonated polymer dispersed in the deuterated host (or vice versa), it is customary to subtract the scattering measured for a random copolymer comprising protonated and deuterated units in the same proportion as in the mixture. In this way, the intensity due to incoherent background scattering is eliminated. Such a procedure subtracts also the "independent scattering" which the monomer units would contribute to the scattering function in the absence of correlations between them. The theoretical scattering function modified accordingly is

$$F_x'(\mu) = F_x(\mu) - \sum_{k,\ell} f_k f_\ell \mu^2 (\mu r_{0;k\ell})^{-1} \sin(\mu r_{0;k\ell}) \Big/ \sum_{k,\ell} f_k f_\ell \quad (2)$$

The scattering function $F_x'(\mu)$ for syndiotactic PMMA obtained by first calculating $F_x(\mu)$ as described above and then subtracting the independent scattering according to eq 2 is shown by the solid curve in Figure 5. The dashed curves labeled "Monte Carlo, C^α" and "g_8" represent scattering functions $F_x'(\mu)$ calculated in the point scatterer approximation. They are obtained from the corresponding

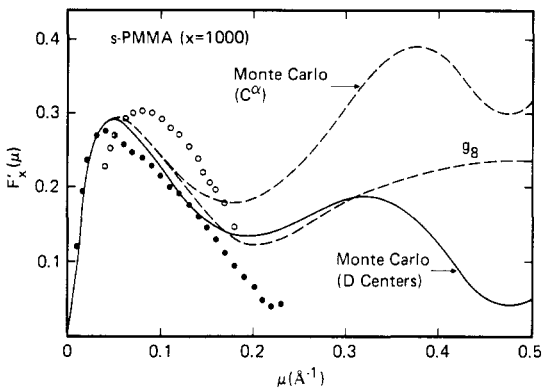

Figure 5. Theoretical scattering functions $F_x'(\mu)$ plotted against μ for syndiotactic PMMA chains of 1000 units. The dashed curves representing the point scatterer approximation are reproduced from Figure 4 after subtracting μ^2; see eq 3. The solid curve represents scattering by protonated groups treated individually according to eq 1 and 2 as described in the text. Filled circles represent neutron scattering results of Kirste, Kruse, and Ibel[4] for predominantly syndiotactic H-PMMA ($\bar{M}_w$ = 250 000, c = 1.19%) dispersed in D-PMMA. Open circles, also from Kirste et al.,[4] represent neutron scattering by a dilute solution of H-PMMA ($\bar{M}_w$ = 34 500) in D-acetone.

curves in Figure 4 by deducting the contribution from the independent scattering by the repeating units. In the point scatterer approximation eq 2 simplifies to

$$F_x'(\mu) = F_x(\mu) - \mu^2 \quad (3)$$

The difference between the two Monte Carlo curves becomes significant beyond μ = 0.10 Å^{-1}, and is large at μ = 0.3 Å^{-1} and beyond. Thus, the effect of resolution of the repeating unit into its principle scattering loci is marked at higher values of μ.

Filled points in Figure 5 represent small-angle neutron scattering results of Kirste, Kruse, and Ibel[4] for predominantly syndiotactic H-PMMA ($w_m \approx 0.2$) at a concentration of 1.19% in D-PMMA, both polymers being of high molecular weight. (The scattering function $F_x(\mu)$ is independent of molecular weight in this range.) The open circles are for a dilute solution of H-PMMA ($w_m \approx 0.2$) in D-acetone.[4] The displacement of the maximum to larger μ for the latter solution may be due to perturbation of the configuration by the effect of excluded volume which is operative in this system. With this qualification, the observed maxima are in excellent agreement with the theoretical calculations represented by the solid curve. The observed data fall below the calculated curve beyond the maximum, indicating a trend toward a lower minimum than the one calculated. However, mounting experimental inaccuracy with increase in μ may have affected the data in this range.

Conclusion

The rotational isomeric state treatment[3] of PMMA gives a remarkably good account of the small-angle x-ray and neutron scattering by this polymer, both in dilute solution and in bulk. The agreement between theory and the experimental results at comparatively large values of μ is especially significant since it confirms the essential correctness of the rotational isomeric analysis as applied to short sequences of units. Thus, the spatial configurations of these short sequences are well represented by the same scheme applicable to the chain as a whole. The conclusions drawn from recent neutron scattering investigations[4,13-16] to the effect that the over-all dimensions of polymer chains dispersed in the bulk amorphous polymers are not perturbed

perceptibly either by intramolecular or by intermolecular interactions therefore hold also for short sequences of units.

Acknowledgment. This work was supported by the National Science Foundation, Grant No. DMR-73-07655 A02.

References and Notes

(1) D. Y. Yoon and P. J. Flory, *Polymer*, **16**, 645 (1975).
(2) D. Y. Yoon and P. J. Flory, *Macromolecules*, preceding paper in this issue.
(3) P. R. Sundararajan and P. J. Flory, *J. Am. Chem. Soc.*, **96**, 5025 (1974).
(4) R. G. Kirste, W. A. Kruse, and K. Ibel, *Polymer*, **16**, 120 (1975).
(5) R. G. Kirste, *Makromol. Chem.*, **101**, 91 (1967).
(6) R. G. Kirste and O. Kratky, *Z. Phys. Chem. (Frankfurt am Main)*, **31**, 363 (1962).
(7) G. Allegra, E. Benedetti, and C. Pedone, *Macromolecules*, **3**, 727 (1970).
(8) T. Tanaka, Y. Chatani, and H. Tadokoro, *J. Polym. Sci., Polym. Phys. Ed.*, **12**, 515 (1974).
(9) P. J. Flory, P. R. Sundararajan, and L. C. DeBolt, *J. Am. Chem. Soc.*, **96**, 5015 (1974).
(10) P. J. Flory, "Statistical Mechanics of Chain Molecules", Interscience, New York, NY., 1969.
(11) P. J. Flory, *Macromolecules*, **7**, 381 (1974).
(12) Y. Fujiwara and P. J. Flory, *Macromolecules*, **3**, 288 (1970).
(13) R. G. Kirste, W. A. Kruse and J. Schelten, *Makromol. Chem.*, **162**, 299 (1972).
(14) H. Benoit et al., *Nature (London), Phys. Sci.*, **245**, 13 (1973).
(15) D. G. Wignall, J. Schelten, and D. G. H. Ballard, *J. Appl. Crystallogr.*, **7**, 190 (1974); *Eur. Polym. J.*, **9**, 965 (1973); **10**, 861 (1974).
(16) G. Leiser, E. W. Fischer, and K. Ibel, *J. Polym. Sci., Polym. Lett.*, **13**, 39 (1975).
(17) The scattering function $I\mu^2$ employed by Kriste, Kruse, and Ibel[4] (see their Figure 6) is the equivalent of $[\bar{M}_w/(X + 1)]F_x(\mu) \approx M_0F_x(\mu)$, where $\bar{M}_w$ is the weight of a monomer unit. Their data have been divided by M_0 = 100 g/mol in order to establish correspondence with our $F_x(\mu)$.

On the Osmotic Second Virial Coefficient of Polymer Solutions

M. Janssens[1] and A. Bellemans*

Université Libre de Bruxelles, Brussels, Belgium. *Received May 27, 1975*

ABSTRACT: The osmotic second virial coefficient A_2 of nonathermal polymer solutions is discussed for a simple lattice model. Each molecule (n-mer) corresponds to a self-avoiding walk of $n - 1$ steps on the simple cubic lattice and each intrachain or interchain contact contributes a quantity $-\epsilon$ to the energy of the system. The function $A_2(n,f)$ where $f = \exp(\epsilon/kT)$ is obtained exactly by direct counting for $n \leq 6$ and is evaluated approximately by a Monte Carlo technique for higher n values up to $n = 40$. In the asymptotic limit $n \to \infty$, it appears that the theta temperature (defined by $A_2 = 0$) is given by $k\Theta/\epsilon \simeq 3.71$ ($f_\Theta \simeq 1.309$) while the quantity $(dA_2/d \ln f)_\Theta$ seems to remain different from zero. Two different theories of polymer solutions are briefly compared to these results.

I. Introduction

The aim of this paper is to investigate the asymptotic form of the second virial coefficient for nonathermal polymer solutions, within the frame of the conventional lattice model. In this sense this paper is the natural continuation of the preceding one,[2a] which was confined to athermal solutions.

Each polymer molecule (n-mer) is represented by a self-avoiding walk occupying n sites of a regular lattice (walk of $n - 1$ steps) and overlap of two such n-mers is forbidden. Empty sites are considered as occupied by solvent molecules (monomers). These n-mers are fully flexible and can assume any configuration on the lattice (provided that overlaps do not occur). An interaction energy $-\epsilon$ is associated to each pair of n-mer segments occupying neighboring sites (provided these segments are not consecutive ones in the same chain).

Putting ϵ equal to zero brings us back to the athermal case, studied previously by McKenzie and Domb[2b] and subsequently by us,[2a] by means of exact enumeration and Monte Carlo sampling, respectively.

We shall limit our considerations to the simple cubic lattice as exemplifying three-dimensional systems. The less relevant two-dimensional case will be studied in a separate paper devoted to the square lattice.

II. Basic Formulas

The second virial coefficient A_2 is related as follows to the osmotic pressure π

$$\pi/kT = \varphi/n + A_2\varphi^2 + \ldots \tag{1}$$

where φ is the fraction of sites occupied by n-mer segments (the volume fraction of n-mers). In terms of the partition functions Z_1, Z_2 relative to one and two n-mers respectively, one has[3]

$$A_2(n,f) = -V(Z_2 - Z_1^2)/2n^2Z_1^2 \tag{2}$$

with

$$Z_s(n,f) = \sum_\nu g_n(V,s;\nu)f^\nu \tag{3}$$

$$f = e^{\epsilon/kT} \tag{4}$$

Here $g_n(V,s;\nu)$ denotes the total number of ways of placing s *distinguishable* nonoverlapping n-mers on a lattice of V sites, such that ν pairs of n-mers segments are in contact.

For a pair of chains ($s = 2$), called respectively 1 and 2, it is convenient to split the total number of contacts ν into ν_i intrachain and ν_e interchain contacts, i.e.,

$$\begin{aligned} \nu &= \nu_i + \nu_e \\ \nu_i &= \nu_{11} + \nu_{22} \\ \nu_e &= \nu_{12} \end{aligned} \tag{5}$$

We then have on account of eq 3

$$Z_2 - Z_1^2 = \sum_{\nu_{11},\nu_{22}} \left[\sum_{\nu_e} g_n(V,2;\nu_{11},\nu_{22},\nu_e)f^{\nu_e} - g_n(V,1;\nu_{11})g_n(V,1;\nu_{22}) \right] f^{\nu_i}$$

which may be rewritten as